DOI: 10.13009/EUCASS2023-997
Aerospace Europe Conference 2023 – 10TH EUCASS – 9TH CEAS

ESD sensitivity analysis of thermites for satellite demise

Filippo Maggi[⋆†] · *Sebastian Manuel Cervelli*[⋆] · *Alessandro Finazzi*[⋆]
[⋆]*Politecnico di Milano*
Via La Masa 34, 20156 Milano, Italy
filippo.maggi@polimi.it · sebastianmanuel.cervelli@mail.polimi.it · alessandro.finazzi@polimi.it

Stefano Dossi[§]
[§]*ReActive Powder Technology S.R.L.*
Via Lambro 7/3, 20068 Peschiera Borromeo, Italy
stefano.dossi@reactivepowders.com

Tobias Lips[•]
[•]*HTG - Hyperschall Technologie Göttingen GmbH*
Am Handweisergraben 13, 37120 Bovenden, Germany
t.lips@htg-gmbh.com

Kobye Bodjona[‡] · *Geert Smet*[‡]
[‡]*ESA-ESTEC*
Keplerlaan 1, 2201 AZ Noordwijk, The Netherlands
kobye.bodjona@esa.int · geert.smet@esa.int ·

[†]Corresponding author

Abstract

In the frame of the SPADEXO project (ESA-TRP), thermites are under evaluation within the design-for-demise (D4D) framework to assist melting of bulky satellite components. This approach, named thermite-for-demise (T4D), consists in installing one or more additional enthalpy sources in precise locations of a satellite. Passive ignition exploiting the aerothermal heat typical of an atmospheric reentry can be assured tailoring thermite properties, driven by composition and, possibly, mechanical activation. In perspective, integration of pyrotechnic charges inside a satellite poses some question about safety, specifically related to the sensitivity of these materials. Whereas the temperature environment does not seem critical during the operative life of a satellite, other aspects have to be considered when handling and storing on-board these energetic materials. In the present paper, the focus is on the characterization of electrostatic discharge (ESD) sensitivity and the general methods used to characterize the minimum ignition energy. The paper addresses the development of a ESD experimental line. Then it critically analyzes the standard methodology used for the definition of the test matrix and the interpretation and reporting of data. From the discussion, the classical Bruceton method and the maximum-likelihood estimator fall short in supplying a comprehensive interpretation of material sensitivity, mainly in the low-end range, which is instead the range where most of attention should be posed for safety limits. The paper proposes a different data organization and interpretation along with some exploratory results of thermites tested within the T4D framework.

1. Introduction

Risks posed by space junk accumulation pushed the space community towards the development of mitigation guidelines, mostly addressing spacecraft end-of-life management. One of the main requirements currently forwarded to space platform developers consists of the 25-year-rule, asking for the removal of the inactive spacecraft within 25 years from its decommissioning. For lower orbits, deorbiting is the preferred option [1]. If the satellite is small enough and the components do not pose specific on-ground risks, an uncontrolled reentry can be considered. Rather, if the casualty risk is too high, the operator is called to perform a controlled reentry, typically consisting in a high thrust maneuver. From a system viewpoint, this causes an increment in complexity, costs, and operational risks. A dedicated propulsion

DOI: 10.13009/EUCASS2023-997

unit and the respective propellant mass budget must be allocated on-board. In addition, the possibility of malfunction has to be taken into consideration.

The casualty risk rules the choice between controlled and uncontrolled reentry, and the survivability of components to the atmospheric reentry maneuver is a key factor. In this respect, within the CleanSpace initiative, the European Space Agency is promoting the development of D4D (design for demise) engineering approach. This wide paradigm consists of several guidelines and methods for the design of new spacecrafts promoting the complete satellite disintegration during reentry. The implementation of D4D approach to critical satellite components can reduce the on-ground casualty risk, allowing the design of a new-generation satellite class compliant with rules for spontaneous reentry and, thus, much less expensive and complex [2, 3]. As reported in Figure 1, the installation of energetic material on satellites is one of the D4D strategies conceived for maximization of available heat. The idea consists of integrating the aero-thermal heating coming from the external reentry environment with additional endogenous enthalpy obtained with some exothermic reaction. In the frame of an ESA-TRP project named SPADEXO, thermites are under investigation to understand their applicability and their potential benefits [4–6].

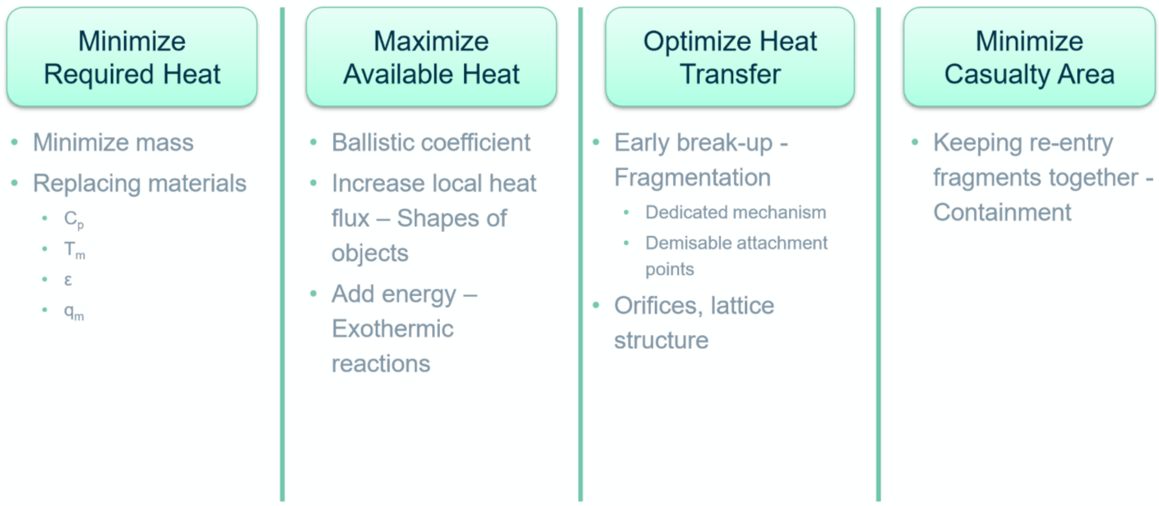

Figure 1: Design for Demise (D4D): different strategies

Thermites are reportedly a class of energetic materials characterized by high energy density and relative handling safety. They are represented by the generic chemical formula reported in Eq. 1. In brief, a metal M^1 and a metal-oxide $M^2_{x2}O_{x3}$ perform an oxygen exchange to generate a new oxide $M^1_{x4}O_{x5}$. A pure metal M^2 is the byproduct of the reaction. The process is strongly exothermic and self-sustained, once the ignition condition is reached [7].

$$M^1 + \frac{x_5}{x_3\,x_4} M^2_{x2}O_{x3} \rightarrow \frac{1}{x_4} M^1_{x4}O_{x5} + \frac{x_2\,x_5}{x_3\,x_4} M^2 \tag{1}$$

Reactant type rules spontaneity of the reaction, enthalpy balance, and ideal reaction products. Size and shape of ingredients, together with their compaction level, are correlated to reaction rate and sensitivity [8–10]. Typically, commercial thermites are obtained by powder mixing of micrometric ingredients. These materials grant relative low sensitivity to these materials. More recently, the introduction of thermites based on nanometric ingredients allowed the production of new energetic materials having behavior comparable to primary explosives used in primer charges. An intermediate class of reactivity is represented by activated thermites. These pyrotechnic materials are obtained by mechanical, chemical, or mechano-chemical process of original ingredients [11, 12]. The advantage of activated thermites consists in the activation process itself. The production methodology is so versatile that grants wide tuning possibility in terms of powder characteristics, such as ignition temperature.

In the perspective of thermites used for D4D applications, we should think of a set of charges attached or embedded in critical parts of the spacecraft. The task of these pyrotechnic devices may span from heating to seizing and the optimal application strategy is still far from being defined. In one embodiment, these devices produce additional heating with respect to the aerothermal contribution and increase the temperature of a component, easing the melting. In another configuration, the exothermic reaction may contribute to the change of shape of critical components, modifying the ballistic coefficient on purpose and enhancing the spontaneous demise. Tuning of ignition temperature becomes of paramount importance to trigger the event at a pre-defined instant of the disposal maneuver and obtain a reproducible and predictable behavior. Spontaneous ignition grants the operating capability even in presence of non-cooperative

DOI: 10.13009/EUCASS2023-997

satellites.

The installation and the presence of these items inside the body of a spacecraft pose several safety concerns. Pyrotechnic devices and explosives are used in the space industry. Solid propellants are 1.3 class explosives and can be found in boosters as well as in separation motors. Pyrotechnic parts can be found in some valves. Linear explosives are used for stage separation [13]. Their safety characterization aims to prevent the unexpected initiation of the exothermal spontaneous decomposition. Typically, a premature ignition may be caused by exposure to heat, friction, impact, electrostatic discharges, shocks, or a combination of them [14]. The same effect may be caused during storage by improper aging of the substance.

The present paper deals with the characterization of the electrostatic discharge sensitivity (ESD) of thermites studied for satellite demise application. Experimental characterizations have demonstrated that both the nature of the ingredients and the particle size are strongly connected to the risk of ignition through spark [15]. In general, the smaller the particles the higher the risk. In this, resistivity of the powder bulk seems to have a role along with the equivalence ratio of the composition, as published by Weir and co-authors [16]. In the same paper, the authors brought as an example the aluminum/copper oxide thermite and demonstrated that the minimum ignition energy (MIE) via ESD can be as low as 5 mJ, far lower than the one needed by thermal ignition.

The paper presents a revised methodology for characterization of sensitivity of energetic materials, here applied to ESD of thermites. The reader will find in Sec. 2 a literature survey on the current standards. In Sec. 3 justification and description of the experimental line is reported. Sec. 4 and following report the methods used in this paper to analyze data and results for two thermite compositions.

2. Background

International standards for ESD sensitivity analysis have been developed both in civil and military frameworks. Typically, studies target the identification of the minimum ignition energy (MIE). In the ESD framework, it represents the smallest electrostatic energetic stimulus that triggers a reaction. Normative and literature cover both experimental phase and data processing (analysis as well as test matrix definition).

2.1 Human body

The human body, as a source of ESD, has been subject of considerations and models, given the intrinsic safety concern on energetic material handling. Kelly and co-authors present an interesting comparison between MIL-STD 883C and other technical papers, discussing about the validity of the implementation suggested by the norm [14]. In general, the paper shows that an equivalent circuit comprises a capacitance in the range 100 pF to 250 pF while the generated voltage discharge may stay between few hundreds of volt up to 30 kV. In a worst case scenario, the energy accumulated by the human body can reach levels of 100 mJ or above.

2.2 Typical experimental approaches

The experimental testing apparatus is not unique. Authors have discussed about the variety of influencing factors on the results of ESD tests. Research groups develop their own apparatuses as well as norms do not show uniform configurations. All of these systems are based on capacitors. Derivation of the energy stored and, then, released by the discharge event on the sample is straightforward, once the operative voltage and the circuit capacitance is known. This set of information can be obtained by a voltage divider and by nominal capacitor data. Uncertainty of both electrical components and of the voltmeter contribute to build up the global uncertainty of the measurement. In some implementation, the discharge is performed through a resistor to simulate a specific current profile. The geometry of the sample holder may differ from case to case. For example, in STANAG 4490 the sample is lodged on the cathode, it is enclosed in a PMMA insulating envelope and the anode is already in contact with the sample. The discharge is commanded by the activation of a contact by the operator. In the European standard EN 13938-2:2004 the sample is confined inside the hole produces in a plastic disk and two copper plates (the electrical leads) cover both ends. Beloni and Dreizin fill with the sample a U-shaped stainless steel cup and place the discharge pin about 0.2 mm above the surface [17]. Lyu and co-authors show two configurations. When a powder is tested, the sample is deposited on the positive lead (anode) while a pin (cathode) is placed 0.5 mm above it. It is interesting to note that the current direction is now reversed with respect to the other cases. When a tablet of explosive is tested, the two electrodes are placed on its surface and the discharge happens at the surface [18].

DOI: 10.13009/EUCASS2023-997

2.3 A common methodology: the Bruceton up-down method

This historical method employed in developing sensitivity estimation follows an *adaptive sampling strategy*. Testing begins at a chosen stress level, leading to either a sample ignition (GO) with a subsequent energy level decrease, or no ignition (NO GO) followed by an energy level increase. The interval between all energy levels is required to be constant and linearly spaced. Alternatively, a logarithmically spaced set of energy levels can be used, granted that the complexity of the problem increases. The Bruceton method is based on the maximum-likelihood estimator of the results of the sensitivity tests (μ) and its standard deviation σ. For this approach, the ignition probability is modeled as the cumulative density function (CDF) of a normal distribution, as reported in Eq. 2.

$$p(E_i) = \frac{1}{\sigma\sqrt{2\pi}} \int_{-\infty}^{E_i} e^{-\frac{(E-\mu)^2}{2\sigma^2}} \, dE \tag{2}$$

Physically speaking, μ represents the energy with an ignition probability of 0.5 (also defined as $E_{50\%}$), which is visibly identified by the point where the cumulative probability density curve changes its concavity. The value of σ dictates the width of the probability density function and influences the steepness of the cumulative curve. In principle, it is expressing how fast the sensitivity is changing around the reference $E_{50\%}$ point.

Despite the simplicity of the formulation, this approach is enforcing the generalized underlying hypothesis that the behavior of the energetic material sensitivity is symmetric with respect to the $E_{50\%}$, towards both the low and the high energy range. Graphically, the cumulative of the probability $p(E)$ follows an S-shaped and symmetric pattern in relation to $p(E_{50\%})$. However, this may not be the case for energetic materials. Additionally, the development of the test matrix following an Up-and-Down generating sequence, as the Bruceton method does, often emphasizes the testing accuracy on energy levels close to $E_{50\%}$, dismissing the importance of the entire range of sensitivity. In this representation the minimum ignition energy (E_{MIE}) does not obtain adequate attention, despite it represents a fundamental safety parameter when dealing with hazardous and explosive materials.

3. ESD experimental line

3.1 Description

The currenty version of the experimental line developed at the Space Propulsion Laboratory, still under refinement, is reported in Fig. 2. It is the result of a three-year-long development process carried on to improve safety and accuracy.

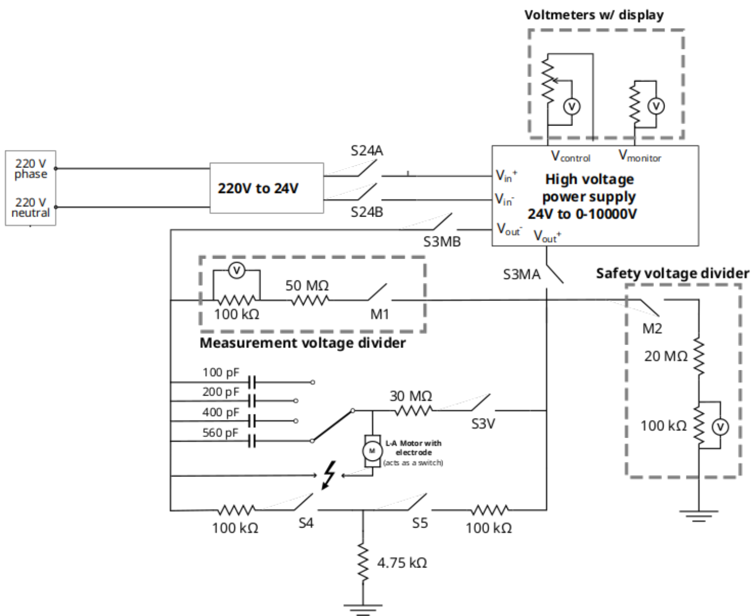

Figure 2

DOI: 10.13009/EUCASS2023-997

Table 1: Capacity of the ESD test circuit as a function of the connected capacitor.

Capacitor id.	Capacitor only	Total capacity
1	100 pF	141 pF
2	200 pF	244 pF
3	400 pF	477 pF
4	560 pF	625 pF

A commercial high-voltage source (Spellman MPS10P10/24, up to 10 kV) is connected to a group of capacitors having capacitance discretely varying in the range 100 pF to 560 pF. A set of switches allows the management of circuit capacity. The test area is made by a metallic sample and a needle-kind electrode. The electrode is lowered by a stepper motor till it touches the sample and, effectively, it acts as a switcher. The monitoring of the generated voltage is performed by a monitoring circuit embedded in the high-voltage source. The connections and the automatic switches create a floating circuit. The sequence of charging, testing, and discharging represents the *testing mode* of the apparatus and is managed by an Arduino Due controller. The system provides also a *measurement mode*, to monitor the generated voltage source using an independent volt meter and an external voltage divider, and a *safety mode*, where the high voltage source is not powered.

3.2 Uncertainty considerations

Accuracy of energy accumulated for discharge is fundamental to define an adequate separation of tested energy levels, given the discrete nature of the apparatus. The energy accumulated in the system E_C depends on the selected charging voltage V_0 and the total capacitance of the circuit C_{tot}, according Eq. 3.

$$E_C = \frac{1}{2} C_{tot} V_0^2 \tag{3}$$

Total capacitance is built up by the capacitor and the circuit. The nature of this experimental line implementation makes circuit capacity non-negligible (see Table 1). Measurement of capacity has been obtained through Aidetek VC97+ multimeter, having a stated accuracy of 2.5 % on the measured value and a resolution of 1 pF. Voltage quantification has been obtained using the internal voltage monitor of the generator. Monitor scale factor is 1000 and declared accuracy is 2 %.

3.3 Definition of energy levels

Capacitor circuiting allows a discrete variation of the value of C_{tot}. The voltage can be changed with continual variation. Correct separation of energy levels permits to distinguish the behavior of tested charges and, thus, to improve accuracy of reactivity identification. Uncertainty analysis focuses on the energy accumulated in circuit capacitance and guides the choice of running parameters to avoid overlaps between adjacent energy intervals due to correlated uncertainty. The Root Sum Squared method (Eq. 4) is applied to identify uncertainty of accumulated energy, discharged on a sample during the *Testing mode*.

$$u_{E_C} = \sqrt{\left(\left.\frac{\partial E_C}{\partial C}\right|_{nom} u_{C_{tot}} \right)^2 + \left(\left.\frac{\partial E_C}{\partial V_0}\right|_{nom} u_{V_0} \right)^2} \tag{4}$$

Whereas the value of voltage uncertainty u_{V_0} is derived from the nominal data sheet of the generator and of its embedded monitoring system, the value of capacitor uncertainty $u_{C_{tot}}$ depends on the measurement accuracy of the global system capacitance. A model based on normal distributions was used to define the separation between two consecutive levels energy adopted during testing. The interval was determined by defining an energy range within which the energy falls, with a certain level of confidence. The level of confidence is uniquely related to the number of standard deviations ($N \cdot \sigma_i$) between the energy level nominal value $E_{C,i}$ (or mean μ_i) and its boundaries. For this purpose, the standard deviation, σ_i, is assumed to be equal to the absolute uncertainty of the i-th energy level, $u_{E_{C,i}}$ [19]. Figure 3 clarifies the concept of separation. Two nominal energy levels E_1 and E_2 are represented with their respective standard deviations $3\sigma_1$ and $3\sigma_2$. The minimum separation between the nominal values granting interval non-overlapping with a probability of 99.73 % is represented by the sum $3\sigma_1 + 3\sigma_2$. The confidence level of the separation can be modified according to Table 2.

DOI: 10.13009/EUCASS2023-997

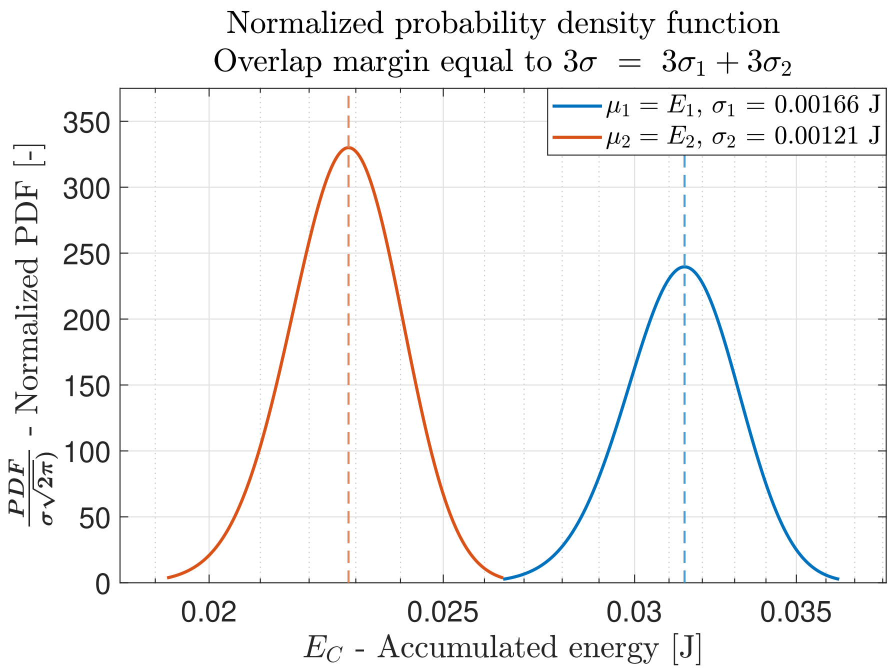

Figure 3: PDF showing the separation of two an overlap bilateral margin equal to $N = 3$ standard deviations

Table 2: Levels of confidence for a separation gap $N \cdot (\sigma_i + \sigma_{i+1})$ between energy levels

N	Energy level range	Separation between energy levels	Level of confidence
1	$E_i \pm 1 \cdot \sigma_i$	$1 \cdot \sigma_i + 1 \cdot \sigma_{i\pm1}$	68.269%
2	$E_i \pm 2 \cdot \sigma_i$	$2 \cdot \sigma_i + 2 \cdot \sigma_{i\pm1}$	95.450%
3	$E_i \pm 3 \cdot \sigma_i$	$3 \cdot \sigma_i + 3 \cdot \sigma_{i\pm1}$	99.730%
4	$E_i \pm 4 \cdot \sigma_i$	$4 \cdot \sigma_i + 4 \cdot \sigma_{i\pm1}$	99.993%
5	$E_i \pm 5 \cdot \sigma_i$	$5 \cdot \sigma_i + 5 \cdot \sigma_{i\pm1}$	99.999%

4. Sensitivity estimation

A fixed-sample test matrix design was employed as an alternative to an $E_{50\%}$-targeting Up-and-Down method (i.e., the Bruceton method). Testing is performed over the entire range of the energetic material sensitivity within the capabilities of the ESD testing machine. Data obtained through this approach ensure the repeatability of experimental campaigns and provide the necessary inputs for conducting a more comprehensive stochastic analysis.

4.1 Normal distribution model

The Bruceton analysis is not compatible with a fixed-sample design, therefore a minimization problem has been formulated to obtain mean, μ, and standard deviation, σ, characterizing the ignition probability. The objective function F (Eq. 5) is the sum over all energy levels of the difference between the estimated ignition probability $p(E_i)$ (Eq. 2) and the observed ignition probability (the ratio of successful ignitions $x_{s,i}$ over the total number of tests n_i at the i-th energy level).

$$F = \sum_{i=1}^{n} \left[\left(p(E_i) - \frac{x_{s,i}}{n_i} \right)^2 \right] \tag{5}$$

The problem aims at finding the values of σ and μ which best fit the experimental cumulative. It is important to emphasize that this model cannot incorporate prior information regarding lower and upper sensitivity boundaries, $[E_l, E_u]$, where $p(E_l) = 0$ and $p(E_u) = 1$, as typically assumed for energetic materials.

DOI: 10.13009/EUCASS2023-997

4.2 Weibull-Model

The Weibull-Model was first introduced in [20] as an alternative to the Bruceton method. The CDF of the Weibull distribution has been re-parametrized to include the sensitivity boundaries. The boundaries are defined as $[E_l, E_u] = [0, +\infty]$ when no prior information is provided.

$$p^{(d_1,d_2)}(E) = \begin{cases} 0 & \text{for } E < E_l \\ \dfrac{1 - e^{-\left(\frac{E-E_l}{d_2}\right)^{d_1}}}{1 - e^{-\left(\frac{E_u-E_l}{d_2}\right)^{d_1}}} & \text{for } E_l \leq E \leq E_u \\ 1 & \text{for } E > E_u \end{cases} \tag{6}$$

The parameters d_1 and d_2 are the two remaining unknowns and confer different shapes to the CDF, as seen in Fig. 4. Concave, convex, and $\boldsymbol{S}$-types are all achievable. This means that the Weibull-Model is able to reflect a broader range of $p(E)$ behavior with respect to the Bruceton method and its underlying model based on the CDF of the normal distribution. See Table 3 for more details.

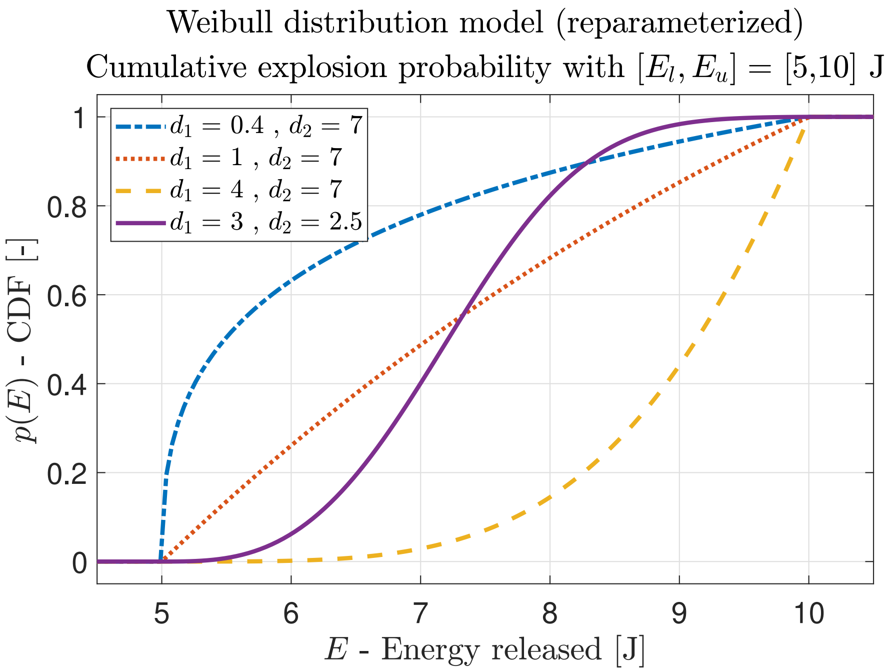

Figure 4: Example of Weibull distribution estimation on the cumulative ignition probability $p(e)$ after reparametrization. Legend order: concave, quasi-linear, convex, $\boldsymbol{S}$-type

The experimental design of the Weibull model relies on the definition of the sample size for each energy level tested (respectively, n_i and E_i), and an arbitrary level of confidence, β. Following the experimental campaign results, the parameters n_i and β, along with the number of "GO" observations for a specific energy level $(x_s|E_i)$, are used to identify the *measurement interval*, $[\underline{p}_{l,i}, \overline{p}_{u,i}]$, which represents the lower and upper boundaries of the estimation of the ignition probability dictated by the so-called measurement space, as defined by Refs. [20, 21] and reported in Table 5 for the specific case of 10 tests ($n_i = 10$). As the sample size grows, the measurement interval shrinks, leading to an increase in accuracy of the estimation. By contrast, a higher level of confidence β is associated to a larger safety margin and measurement interval. According to the Least Squared Error approach, a minimization problem searches for the values of d_1 and d_2 minimizing the cost function J with two boundary conditions enforced for the lower and upper end of the energy level interval (respectively, E_l and E_u) according to Eq. 7.

$$\begin{cases} p(e_l) = 0 \\ J = \sum_{i=1}^{n} \left[\left(p(E_i) - \underline{p}_{l,i}\right)^2 + \left(p(E_i) - \overline{p}_{u,i}\right)^2 \right] \\ p(e_u) = 1 \end{cases} \tag{7}$$

DOI: 10.13009/EUCASS2023-997

Table 3: $p(E)$ behaviour with different values of d_1 and d_2 [20]

$(d_1, d_2) \in (...)$	**Type**	**Sensitivity**
$0 < d_1 \leq 1, 0 < d_2$	**Concave**	Strong growth near E_l
$1 < d_1, (E_u - E_l)\left(\frac{d_1}{d_1-1}\right)^{\frac{1}{d_1}} \leq d_2$	**Convex**	Strong growth near E_u
$1 < d_1, 0 < d_2 < (E_u - E_l)\left(\frac{d_1}{d_1-1}\right)^{\frac{1}{d_1}}$	***S*-Type**	Moderate behavior
Boundary cases	**- Quasi-linear behavior** **- Step function alike**	Flexible behavior

5. Results

The ESD testing machine was used to evaluate the sensitivity of Al/Bi_2O_3, and Al/MoO_2 activated micrometric thermites. The sample size consisted of 30 mg, with ten tests for each energy level. The results of the experimental campaign were overall consistent with the formulation of a monotonically increasing sensitivity as the stimulus level is increased. Figure 5 compares the results of the two estimation models, the Normal distribution and the Weibull-Model with level of confidence $\beta = 95$ % and no prior information on $[E_l, E_u]$.

Both models tend to identify similar data for the the $E_{50\%}$ and correctly highlight higher reactivity of the Al/Bi_2O_3 thermite with respect to the Al/MoO_2 composition.

The Weibull-Model was capable of providing a realistic ignition probability curve starting from $p(0) = 0\%$, with a realistic asymptotic behavior. On the contrary, the Normal distribution model resulted in probability of ignition $p(E) > 0\% \ \forall E \in [0, +\infty)$ due to the formulation of the CDF.

The coefficient of determination R^2 has been used to measure the goodness of fit of the different models, i.e. how related the estimations of the ignition probability $p(E_i)$ is to the observed probabilities $\frac{x_s|E_i}{n_i}$. The results are listed in Table 4. While the Weibull-Model results in the worst fitting among the different methods, it is important to remind that this estimation is heavily affected by the sample size and the level of confidence β, whereas the Normal distribution model fails to provide a fully meaningful input and output to determine the sensitivity boundaries of the charges, especially at the edges of the test interval. Furthermore, when providing the estimation problem with lower and upper sensitivity boundaries information ($[E_l, E_u]$), e.g. by extensive testing or prior knowledge, the Weibull-Model shows a significant improvement in R^2. In that table, $E_{test-min}$ indicates the minimum energy level used for tests and resulting in no ignitions while $E_{test-max}$ represents the maximum tested value, granting 100 % probability of events. Further experiments and respective analysis are contained in Ref. [22].

6. Final remarks

The present paper has discussed the problems related to sensitivity experimental analysis and data manipulation. The test apparatus demonstrated to work properly and has been put in full operation. The work discussed the problems related to the use of the Bruceton method for the test matrix development and to the limitations in using a Normal distribution model to analyze the outcomes. The proposed approach tries to overcome both limits. The presented results show that, on an global perspective, the current Weibull-Model version is still less accurate in data representation than the Normal distribution one, but it allows better ignition probability representation at the extreme sides of the test interval. The activity is progressing in the development of an improved Weibull-Model with a more refined approach for better data representation, trying to surpass the concept of measurement spaces.

DOI: 10.13009/EUCASS2023-997

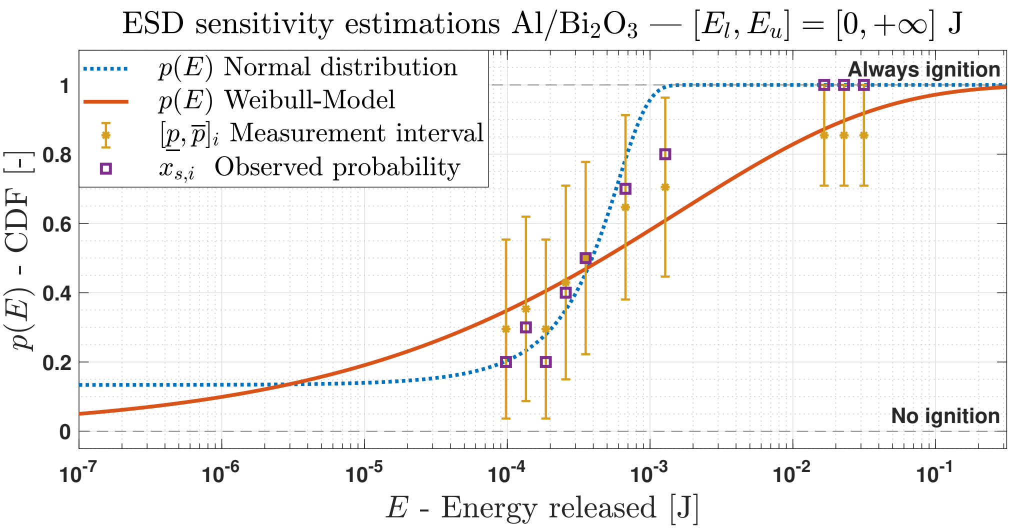

(a) Micrometric Al/Bi_2O_3 thermite activated for 7 minutes

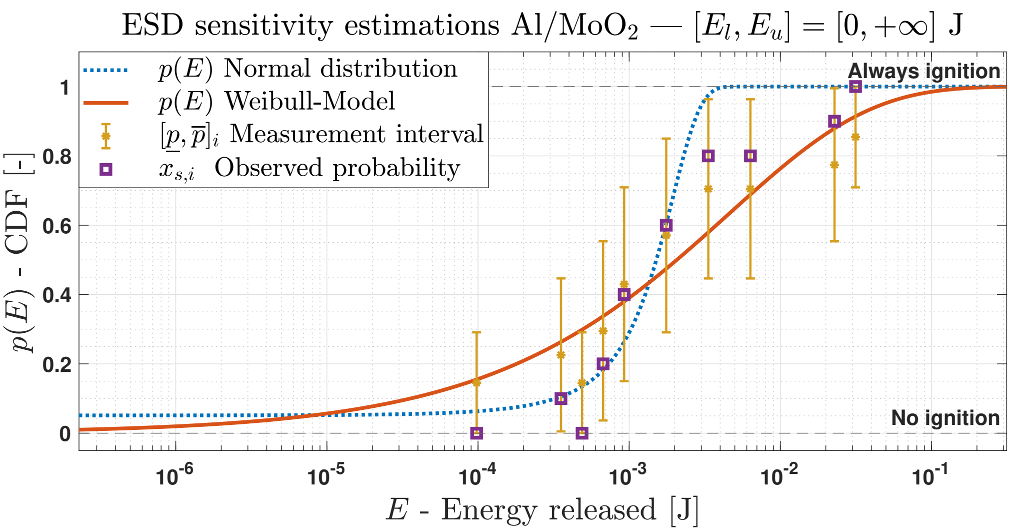

(b) Micrometric Al/MoO_2 thermite activated for 10 minutes

Figure 5: Comparison of the ignition sensitivity estimation models

Table 4: Comparison of coefficients of determination R^2 of the estimation models

R^2	Al/Bi_2O_3	Al/MoO_2
Weibull-Model $[E_l, E_u] = [0, +\infty]$	0.8296	0.8202
Weibull-Model w/ bounds $[E_l, E_u] = [0, E_{test-max}]$	0.9460	-
Weibull-Model w/ bounds $[E_l, E_u] = [E_{test-min}, E_{test-max}]$	-	0.8891
Normal distribution model	0.9393	0.9101

DOI: 10.13009/EUCASS2023-997

Table 5: Weibull-Model measurement spaces for $n_i = 10$, extracted from Ref. [21]

n_i	β		x_s										
			0	1	2	3	4	5	6	7	8	9	10
10	80%	$\underline{p}_l$	0.0000	0.0220	0.0832	0.1576	0.2080	0.3085	0.3868	0.4511	0.5488	0.6914	0.7919
		$\overline{p}_u$	0.2081	0.3086	0.4512	0.5489	0.6132	0.6915	0.7920	0.8424	0.9168	0.9780	1.0000
	95%	$\underline{p}_l$	0.0000	0.0051	0.0367	0.0872	0.1500	0.2224	0.2908	0.3805	0.4464	0.5535	0.7091
		$\overline{p}_u$	0.2909	0.4465	0.5536	0.6195	0.7092	0.7776	0.8500	0.9128	0.9633	0.9949	1.0000
	99%	$\underline{p}_l$	0.0000	0.0010	0.0155	0.0475	0.0932	0.1504	0.2183	0.2971	0.3832	0.4876	0.6167
		$\overline{p}_u$	0.3833	0.5124	0.4512	0.6168	0.7029	0.7817	0.8496	0.9068	0.9525	0.9990	1.0000

DOI: 10.13009/EUCASS2023-997

7. Acknowledgments

This work is part of the activity ”Low environmental impact technology solutions for space access”, performed within the ”MUSA - Multilayered Urban Sustainability Action” project, funded by the European Union - NextGenerationEU, under the National Recovery and Resilience Plan (NRRP) Mission 4 Component 2 Investment Line 1.5 (Strengthening of research structures and creation of R&D ”innovation ecosystems”, set up of ”territorial leaders in R&D”).

The authors acknowledge the collaboration of ReActive Powder Technology S.R.L. company which supplied the activated powders thanks to the support of the SPADEXO project, a TRP project of the European Space Agency, Contract No. 4000136082/21/NL/MG.

References

[1] AA.VV. IADC space debris mitigation guidelines. Technical Report Revision 2, Inter-Agency Space Debris Coordination Committee, 2020.

[2] AA.VV. DIVE - guidelines for analysing and testing the demise of man made space objects during re-entry. Technical Note ESA-TECSYE-TN-018311, European Space Agency, 2020.

[3] AA.VV. ESA space debris mitigation compliance verification guidelines. Technical Report ESSB-HB-U-002, Issue 1, Revision 0, European Space Agency, ESA Space Debris Mitigation WG, 2015.

[4] R. Seiler and G. Smet. Exothermic reaction aided spacecraft demise during re-entry (Patent EP 3604143A1), 2018.

[5] D. Dihlan and P. Omaly. Element de vehicule spatial a capacite d'autodestruction amelioree et procede de fabrication d'un tel element (Patent FR 2975080B1), 2011.

[6] K. Monogarov, A. Pivkina, L. Grishin, Y. V. Frolov, and D. Dilhan. Uncontrolled re-entry of satellite parts after finishing their mission in LEO: Titanium alloy degradation by thermite reaction energy. *Acta Astronautica*, 135:69–75, 2017.

[7] S. Fischer and N. Grubelich. Theoretical energy release of thermites, intermetallics, and combustible metals. In *24th International Pyrotechnics Seminar*, 1998.

[8] M. L. Pantoya. Final report: Combustion and ignition studies of nanocomposite energetic materials. Technical Report 45696-EG-PCS.24, Texas Technical University, Lubbock, TX, 2010.

[9] M. L. Pantoya and J. J. Granier. Combustion behavior of highly energetic thermites: Nano versus micron composites. *Propellants, Explosives, Pyrotechnics*, 30(1):53–62, 2005.

[10] D. Stamatis and E. L. Dreizin. Thermal initiation of consolidated nanocomposite thermites. *Combustion and Flame*, 158(8):1631–1637, 2011.

[11] C. Suryanarayana. Mechanical alloying and milling. *Progress in Materials Science*, 46:1–184, 2001.

[12] S. Dossi, C. Paravan, F. Maggi, and L. Galfetti. Enhancing micrometric aluminum reactivity by mechanical activation. In *Innovative Energetic Materials: Properties, Combustion Performance and Application*, pages 17–44. Springer Singapore, 2020.

[13] J. Fritz. Separation joint technology. In *39th AIAA/ASME/SAE/ASEE Joint Propulsion Conference and Exhibit*, number 2003-4436. American Institute of Aeronautics and Astronautics, 2003.

[14] M. Kelly, G. Servais, and T. Pfaffenbach. An investigation of human body electrostatic discharge. In *International Symposium For Testing And Failure Analysis*, pages 167–167. 1993.

[15] D. Kelly, P. Beland, P. Brousseau, and C. F. Petre. Electrostatic discharge sensitivity and resistivity measurements of al nanothermites and their fuel and oxidant precursors. *Central European Journal of Energetic Materials*, 14(1):105–119, 2017.

[16] C. Weir, M. L. Pantoya, G. Ramachandran, T. Dallas, D. Prentice, and M. Daniels. Electrostatic discharge sensitivity and electrical conductivity of composite energetic materials. *Journal of Electrostatics*, 71(1):77–83, 2013.

DOI: 10.13009/EUCASS2023-997

[17] E. Beloni and E. L. Dreizin. Experimental study of ignition of magnesium powder by electrostatic discharge. *Combustion and Flame*, 156(7):1386–1395, 2009.

[18] Z. Lyu, X. Long, Z. Li, X. Dai, M. Li, K. Yao, C. Deng, and Y. Wen. Different ignition responses of powdery and bulky 1,3,5-triamino-2,4,6-trinitrobenzene (TATB) based polymer-bonded explosives under ultra-high voltage electrostatic discharge. *Central European Journal of Energetic Materials*, 15(2):283–298, 2018.

[19] BIPM, IEC, IFCC, ILAC, ISO, IUPAC, IUPAP, and OIML. Evaluation of measurement data — An introduction to the "Guide to the expression of uncertainty in measurement" and related documents. Joint Committee for Guides in Metrology, JCGM 104:2009, 2009.

[20] R. Wild and E. von Collani. Modelling of explosives sensitivity part 2: The weibull-model. *Economic Quality Control - Econ Qual Contr*, 17:195–220, 01 2002.

[21] E. von Collani and K. Dräger. *Binomial Distribution Handbook for Scientists and Engineers*. Birkhäuser, 01 2001.

[22] S. M. Cervelli. Investigation of esd sensitivity in energetic materials: mathematical models and experimental design. Master's thesis, M.Sc. Thesis, Politecnico di Milano, 2023.